HOKKAIDO UNIVERSITY

Title	In-Frame Deletion Mutant of eIF4E1 Attenuates Cucumber Mosaic Virus Virulence by Interfering With 2b Function in Tomato
Author(s)	Ghos, Sozib; Kawakubo, Ayaka; Akhter, Md Shamim et al.
Citation	Physiologia Plantarum, 177(4) https://doi.org/10.1111/ppl.70369
Issue Date	2025-07
Doc URL	https://hdl.handle.net/2115/97971
Rights	The definitive version is available at onlinelibrary.wiley.com
Type	journal article
File Information	PPL-2025-00526_Husca.pdf

Hokkaido University Collection of Scholarly and Academic Papers : HUSCAP

In-frame deletion mutant of eIF4E1 attenuates cucumber mosaic virus virulence by interfering with 2b function in tomato

Sozib Ghos[1†] | Ayaka Kawakubo[1†] | Md Shamim Akhter[1,2] | Akinori Yoshimura[1] | Miyuki Suto[1] | Kami Murakami[1] | Chiaki Konishi[3] | Hiroki Atarashi[3] | Kenji S. Nakahara[1,*]

[1] Research Faculty of Agriculture, Hokkaido University, Sapporo, Japan

[2] Bangladesh Agricultural Research Institute (BARI), Bangladesh

[3] Research and Development Division, Kikkoman Corporation, Noda, Japan

† These authors contributed equally to this work.

ORCIDs

Kenji S. Nakahara https://orcid.org/0000-0002-9541-3208

Md Sharmim Akhter https://orcid.org/0000-0003-1632-8783

Sozib Ghos https://orcid.org/0009-0004-4705-2104

***Correspondence**

Kenji S. Nakahara

Email: knakahar@agr.hokudai.ac.jp

Edited by M.T Islam

Abstract

The eukaryotic translation initiation factor 4E (eIF4E) family is essential for host gene expression and is also exploited by certain viruses for viral replication. Mutations in plant eIF4E genes disrupt their interactions with viral proteins and confer resistance to various viruses. Previously, we showed that CRISPR/Cas9-edited tomato plants with a 9-nucleotide deletion (*9DEL*) in the eIF4E1 coding sequence exhibited enhanced resistance to cucumber

mosaic virus (CMV). Here, we investigated the underlying mechanism of this resistance. We found that both wild-type and 9DEL-eIF4E1 proteins bind to the CMV 2b protein. 2b is a multifunctional protein, and our results indicate that its binding to eIF4E1 at least interferes with its RNA silencing suppression activity. In inoculation tests, CMV lacking 2b failed to establish systemic infection in tomato plants but retained the ability to establish systemic infection in *N. benthamiana*, indicating that targeting 2b is more effective in tomato. Our data suggest that *9DEL*-mediated CMV resistance arises from a modified function of 9DEL-eIF4E1, which interferes with the activity of CMV 2b. This study is the first to demonstrate the interaction between eIF4E and CMV 2b.

KEYWORDS: eIF4E1, cucumber mosaic virus, 2b protein, RNA silencing suppressor.

1 | INTRODUCTION

Cucumber mosaic virus (CMV) belongs to the genus *Cucumovirus* in the *Bromoviridae* family, is a well-known pathogen infecting various plant species, including tomatoes, posing an enormous threat to global agriculture (Tatineni and Hein 2023). It ranks as the fourth most significant among all plant viruses (Scholthof et al. 2011), transmitted primarily by aphids and occasionally via seeds, and the symptoms of CMV infection encompass a mosaic pattern, stunted growth, chlorosis, dwarfing, leaf malformation, systemic necrosis, and death (Pagán 2019; Hirsch and Moury 2021). The CMV genome has three segments (RNA1, RNA2, and RNA3), along with two sub-genomic RNAs (RNA4 and RNA4A). CMV encodes five proteins: 1a, 2a, 3a (movement protein), and 3b (coat protein) translated from RNA1, RNA2, RNA3, and sub-genomic RNA4, respectively. The 2b protein is encoded by RNA2 but is translated from the sub-genomic RNA4A at the 3′ end of RNA2 (Palukaitis 2019). It is a multifunctional virulence determinant that affects host gene expression, increases viral accumulation, and aids in viral movement within the plant (Lewsey et al. 2009; Crawshaw et al. 2024). The 2b proteins of CMV variants, including R2b, Y2b, and HL2b, differ in amino acid sequences, which can affect their RSS activity and pathogenicity. For example, A2b (CM95) and R2b (CM95R) differ by a single amino acid at the position 46 (C to R), while Y2b shares a significantly similar sequence with R2b but contains unique substitutions, and the HL2b (from lily strain) induces necrotic spots on infected *Arabidopsis*, unlike subgroup l strains like CMV-Y (Goto et al. 2007; Sueda et al. 2010; Masuta et al. 2012; Kim et al. 2022). In contrast, 2b from CMV(Ho) mutant, belonging to

subgroup IA, has been reported to be asymptomatic in *Arabidopsis thaliana*, suggesting that even minor sequence changes in 2b can result in substantial differences in symptoms (Takahashi et al. 2022). These sequence variations may affect its interaction with host factors, modulating CMV virulence and symptom induction.

The functional importance of the 2b protein varies among host plant species, highlighting differences in host-virus interactions. In *Arabidopsis thaliana*, 2b binds to ARGONAUTE 1 (AGO1), suppressing RNA silencing and increasing CMV accumulation and virulence (Zhao et al. 2018). It also interacts with CAT3, impairing its function and leading to necrosis and enhanced viral accumulation (Murota et al. 2017). In *Nicotiana benthamiana*, 2b interacts with ribosomal protein S11 (RPS11) to promote CMV replication and RNA silencing suppressor (RSS) activity, essential for infection (Wang et al. 2017). Additionally, it binds to HSP90s, preventing SA-induced degradation of NPR3, thereby inhibiting NPR1 activation and suppressing SA-mediated defense (Zhang et al. 2024). In *Nicotiana tabacum*, 2b enhances systemic infection and symptom severity by suppressing RNA silencing, but CMVΔ2b can still achieve systemic infection, indicating that 2b is not essential (Sunpapao et al. 2009). In tomato, 2b disrupts RNA silencing and modulates both salicylic acid (SA) and jasmonic acid (JA) signaling pathways, promoting systemic CMV infection and symptom severity (Khaing et al. 2020a). It suppresses SA-mediated defense by stabilizing NPR3 while inhibiting NPR1, leading to reduced *PR1* gene expression and increased susceptibility (Zhang et al. 2024). Furthermore, 2b disrupts JA signaling by binding to AGO1, interfering with JA-responsive genes such as *PDF1.2* and *VSP2*, weakening plant defenses against herbivores and pathogens (Arinaitwe et al. 2023; Crawshaw et al. 2024). It also interacts with jasmonate ZIM-domain (JAZ) proteins, preventing *COI1*-mediated degradation of JAZ, thereby enhancing aphid attraction and facilitating virus transmission (Wu et al. 2017). The C-terminal region of 2b is crucial for suppressing SA-mediated defenses and ensuring efficient CMV systemic infection (Zhou et al. 2014).

Viruses rely on host susceptibility factors for their proliferation; such factors include eukaryotic translation initiation factor 4E (eIF4E), which is essential for initiating translation in eukaryotes. Mutations in eIF4E disrupt its interaction with viral genome-linked proteins (VPg), conferring resistance to multiple viruses including potyviruses. Natural eIF4E mutations, such as *D55G* in tobacco, confer resistance to potato virus Y (PVY), while *D71G* in watermelon disrupts the VPg–eIF4E interaction, conferring resistance to papaya ringspot virus-watermelon strain (PRSV-W), zucchini yellow mosaic virus (ZYMV), and watermelon mosaic virus (WMV) (Zhou et al. 2024). Similarly, the natural mutation *Ala64Val* in sugarcane eIF4E prevents interaction with the VPg, impairing viral

replication and conferring resistance to sugarcane streak mosaic virus (SCSMV) (Shan et al. 2023). The advances in genome editing techniques such as CRISPR/Cas9 and TILLING allow targeted modifications in eIF4E, mostly resulting in gene knockouts, disrupting interaction with viral proteins and providing an effective strategy for developing crops with robust resistance to multiple potyviruses. CRISPR/Cas9 editing of *eIF4E* conferred resistance to many potyviruses, including pepper mottle virus (PepMoV), clover yellow vein virus (ClYVV), and pepper veinal mottle virus (PVMV) (Bastet et al. 2019; Moury et al. 2020; Yoon et al. 2020; Kuroiwa et al. 2022). TILLING-induced mutations eliminated the expression of eIF4E, preventing its interaction with a viral protein and conferring resistance to PVY and PepMoV; however, gene redundancy may affect the resistance (Piron et al. 2010; Gauffier et al. 2016). RNAi-mediated silencing of *eIF4E1* and *eIF4E2* reduced the viral interaction and virus accumulation, providing broad-spectrum resistance to potyviruses such as PVY, PepMoV, tobacco etch virus (TEV), soybean mosaic virus (SMV), bean common mosaic virus (BCMV), and watermelon mosaic virus (WMV) though at the cost of impaired plant growth (Mazier et al. 2011; Gao et al. 2020). These studies highlight *eIF4E* as a key target for developing virus-resistant crops; yet, its knockout, while conferring resistance, may negatively impact plant growth.

Previously, we have created CRISPR-Cas9-edited tomato plants carrying three alleles: with 3- or 9-nucleotide deletions (*3DEL* and *9DEL* plants) or a point insertion (*1INS* plants) in the second half of the *eIF4E1* coding region (Atarashi et al. 2020). The *1INS* mutation falls in the class of the Knockout genes in *1INS* plants, no functional protein is produced, because of a frameshift caused by the 1-nucleotide deletion in the first exon. *1INS* plants are resistant to one of the two PVY strains tested, but not to CMV. In contrast, the *9DEL* plants are susceptible to PVY but are partially resistant to CMV, making it an unusual *eIF4E* resistance allele. Inoculation of *1INS* tomato suggested that eIF4E1 is needed for PVY but not for CMV infection. Since eIF4E1 retains its function for tested PVY infection, we assumed that the mutated eIF4E1 protein in *9DEL* tomatoes (9DEL-eIF4E1) has gained inhibitory activity against CMV infection (Atarashi et al. 2020).

In this study, we investigated the mechanism behind the *9DEL* partial resistance to CMV. We hypothesized that 9DEL-eIF4E1 interacts with CMV protein(s). Using the yeast two-hybrid (Y2H) assay, we identified 2b as an interactive partner for 9DEL-eIF4E1. Further experiments suggested that this binding inhibits 2b function, and we suggest that *9DEL*-mediated partial inhibition of 2b suppressor activity could explain the plant partial resistance to CMV.

2 | MATERIALS AND METHODS

2.1 | Plant and virus materials

Tomato (*Solanum lycopersicum* L.) 'S8', *9DEL* (derived from 'S8'; Atarashi et al. 2020), 'Moneymaker', and *N. benthamiana* were used. Plants were grown in a growth chamber at 25℃ under a 16-h light / 8-h dark cycle. *N. benthamiana* leaves infected with CMV-Yellow strain (CMV-Y; Kataoka et al. 1990), its artificial mutant CMVΔ2b, lacking the 2b protein (Matsuo et al. 2007), and its truncate CMV-2bΔC, lacking the C-terminal region of 2b (Otagaki et al. 2006), were the source of inoculum used in inoculation tests. CMV-Y was the source of Y2b (Kataoka et al. 1990), CMV-R95 of R2b (Goto et al. 2007), and lily-derived strain CMV-HL of HL2b (Masuta et al. 2012). Viruses carrying the mutant variants of 2b proteins created by site-specific mutagenesis were used (Ryabov et al. 2001; Tungadi et al. 2017).

2.2 | Plasmids for Y2H assay

DNA fragments encoding 9DEL-eIF4E1 of *9DEL* plants and eIF4E1 of 'S8' were cloned into the pGADT7 vector (Atarashi et al. 2020), and those for CMV proteins, CP (Palukaitis et al. 1992), MP (Suzuki et al. 1991), and 2bs of two different strains (R2b and HL2b) were cloned into the GBT9 vector. To introduce mutations in cloned target sequences in pGADT7 or pGBT9 vectors, inverse PCR amplification was performed using the KOD One™ PCR Master Mix Blue (Toyobo) as follows: an initial denaturation at 94°C for 2 min, 30 cycles of denaturation at 98°C for 10 s, annealing at 60°C for 30 s, and extension at 68°C for 6 min, and a final extension at 72°C for 3 min. The PCR products were digested with *Dpn*I and purified using a MonoFas® DNA purification Kit l. *T4* DNA ligase (Promega) was used for ligation at 16°C for 30 min, and the ligation mixture was transformed into *E. coli* DH5α cells using heat shock at 42℃ for 30 s and chilling on ice for 2 min. Transformants were analyzed by colony PCR (GoTaq®) and sequenced. All primers are listed in Table S1.

2.3 | Y2H assay

The Matchmaker™ GAL4 Two-Hybrid System 3 (Clontech Laboratories) was used, following the manufacturer's protocols. The *Saccharomyces cerevisiae* Y2HGold strain was cultivated in liquid YPAD medium at 30℃ overnight with continuous agitation. The pellets were harvested by centrifugation at 3000 ×*g* for 5 min, washed twice with distilled water, centrifuged at 3000 ×*g*, resuspended in 1 mL of 100 mM lithium acetate, and incubated at room

temperature for 10 min. Transformation solution (360 µL per sample) contained 240 µL of 50% PEG-3350, 36 µL of 1 M lithium acetate, 5 µL of 10 mg ml^{-1} *SSS* DNA (Salmon Sperm DNA), 36 µL of DMSO, and nuclease-free water; to this mixture, 100 µL of yeast suspension and 1 µL of respective plasmid DNA were added. The mixture was incubated for 30 min each at 30℃ and 42℃, and centrifuged at 3000 ×*g* for 5 min. The pellets were resuspended in 500 µL of nuclease-free water and spread on selective SD media lacking Leu/Trp (SD-LT), Leu/Trp/His (SD-LTH), or Leu/Trp/His/Ade (SD-LTHA). Plates were incubated for 3–4 days at 30℃. Protein interactions were evaluated as previously described (Mehla et al. 2015; Yu et al. 2020).

2.4 | Agrobacterium transformation and infiltration

Agrobacterium tumefaciens LBA4404 competent cells (Takara Bio Inc.) were thawed on ice. They were mixed with 300–500 ng of binary vector DNA, incubated on ice for 15–30 min, chilled in liquid nitrogen for 20 s, and incubated at 37°C for 5 min. Pre-warmed SOC medium (900 µL) was added; the mixture was incubated at 28°C for 4 h with gentle shaking and centrifuged at 5000 ×*g* for 3 min. The pellets were resuspended in the remaining medium. Bacterial suspension was spread onto LB plates with appropriate antibiotics (kanamycin, streptomycin, rifampicin, hygromycin) for selection. The plates were incubated at 28°C for 2–3 days. Selected colonies were cultured in 4 mL LB broth supplemented with appropriate antibiotics (25 µL of a 50 mg mL^{-1} stock solution of each) and incubated at 28°C with gentle shaking for 48 h. The suspension was centrifuged at 4000 ×*g* for 10 min; the pellets were resuspended in infiltration buffer (10 mM $MgCl_2$, 10 mM MES, 24 µL of Acetosyringone) and incubated at room temperature. The abaxial surface (underside) of *N. benthamiana* leaves was inoculated using a needleless plastic syringe loaded with the suspension. Inoculated plants were maintained at 25°C at 16 h light / 8 h darkness.

2.5 | Split luciferase complementation assay

The Split-Luc assay was performed as previously described (Chen et al. 2008a; Zhou et al. 2018). Binary vectors were constructed to express PVX CP and R2b fused to N-terminal fragment of luciferase (nLuc), while C-terminal fragment (cLuc) fused to R2b, eIF4E1, and 9DEL-eIF4E1, under the control of CaMV 35S promoter. The co-infiltrated combinations were R2b x PVX CP, 9DEL-eIF4E1 x R2b, 9DEL-eIF4E1 x PVX CP, R2b x R2b (as a positive control), eIF4E1 x R2b, and eIF4E1 x PVX CP, where PVX CP combinations served as a negative control. *N. benthamiana* leaves were co-infiltrated as described above, and the plants were maintained at 25°C at 16 h light /

8h darkness for 35 to 38 h. Infiltrated leaves were sprayed with 1 mM D-luciferin solution and incubated in darkness for 7 min. The chemiluminescence luciferase signals were detected using the FUJIFILM Luminescent Image Analyzer LAS-4000mini (FUJIFLIM Corporation), and the luciferase intensity (Integarted Density) was quantified using ImageJ.

2.6 | Western blotting

Total protein was extracted from 25 mg of infiltrated leaves that were crushed in liquid nitrogen and suspended in 10 times 1% SDS-PAGE Laemmli's sample buffer (0.5 M Tris·HCl pH 6.8, 10% glycerol, 5% mercaptoethanol, 1% SDS, 0.01% Bromophenol blue). The mixture was homogenized, denatured at 95°C for 5 min, and centrifuged at 14000 ×*g* for 5 min at 4°C. Western blot was performed as described previously (Kuroiwa et al. 2022) with antisera against eIF4E1 and eIF4E2 (Gauffier et al. 2016).

2.7 | Total RNA extraction

Total RNA was extracted using TRIzol™ Reagent (Thermo Fisher Scientific). All centrifugation steps were performed at 14000 ×*g* for 15 min at 4°C unless specified otherwise, and all incubation steps were performed at room temperature. Infiltrated leaf tissue (50 mg) was collected at 3 days post-infection (dpi), crushed in liquid nitrogen, homogenized in 1 mL Trizol, and incubated for 5 min. Chloroform (100 µL) was added; the mixture was vortexed for 5 min, incubated for 3 min, and centrifuged. The aqueous phase was added to 250 µL of 2-propanol, incubated for 10 min, and centrifuged. The pellet was washed with 1 mL of 70% ethanol, centrifuged for 3 min, air dried for 5 min, and resuspended in 200 µL of RNase-free water. Phenol and chloroform (100 µL each) were added; the mixture was vortexed for 5 min and centrifuged. The aqueous phase was transferred into a new tube, and RNA was precipitated by adding sodium acetate (0.1 volume; 5 M, pH 5.2, adjusted with acetic acid) and 100% ethanol (2.5 volume) and centrifugation. The pellet was washed and centrifuged as above, air-dried for 5–10 min, and resuspended in 50 µL RNase-free water.

2.8 | cDNA preparation

Total RNA (25 µL), 3 µL of 10× DNase1 incubation buffer, 1 µL of DNase1, and 0.5 µL of RNase inhibitor were mixed and incubated at 37°C for 30 min. Nuclease-free water (200 µL) and phenol:chloroform (100 µL each) were

added; the mixture was vortexed for 1 min and then centrifuged at 14000 ×*g* for 3 min. The aqueous phase (200 μL) was mixed with 20 μL of 3 M sodium acetate (pH 5.0) and 500 μL 100% ethanol; the mixture was vortexed and then centrifuged at 14000 ×*g* for 5 min. The pellet was washed in 1 mL 70% ethanol and centrifuged at 14000 ×*g* for 3 min. The pellet was air-dried for 5–10 min and dissolved in 25 μL of nuclease-free water, and the mixture was boiled for 2 min. Reverse transcription reaction mixture (20 μL) contained 2–3 μL (0.5–5 μg) of denatured total RNA, 0.5 μL of the random primer, 4 μL of 5× buffer, 2 μL of 10 mM dNTP, 0.5 μL of RNase inhibitor, nuclease-free water, and 1 μL of ReverTraAce. The mixture was incubated at 30℃ for 10 min, 42℃ for 30 min, and 99℃ for 5 min.

2.9 | Quantitative RT-PCR

Quantitative RT-PCR was performed with three independent biological replicates per sample. The PCR mixture (10 μL) contained 5 μL of Thunderbird® Next SYBR™ qPCR Mix (Toyobo Co., Ltd.), 0.15 μL of each forward and reverse primer, 1 μL of cDNA, and nuclease-free water. The primers were designed from the NCBI database sequences (a) for eIF4E1 and 9DEL-eIF4E1 (5′-ATGGAACAGAAACTGATCTCTGAAG-3′ and 5′-AGTTCATCGTCTACCTCTCCTCCTC-3′), (b) for R2b (5′-ATGGAATTGAACGTAGGCGCGATGA-3′ and 5′-ACTTTTGTGACCTCGTTCCCGTCGA-3′), (c) for GFP (5′-ATGAGTAAAGGAGAAGAACTTTTCAC-3′ and 5′-TCCGTATGTTGCATCACCTTCACCC-3′); the NbL23areal seq primer pair (5′-CATTGTTGATCTCAAAGCTGACAAG-3′ and 5′-GAACAAACGCCTTCTTGGTTCCATC-3′) was used as a control. PCR amplification was performed as follows: initial denaturation at 95°C for 2 min, 40 cycles of denaturation at 95°C for 5 s, annealing at 60°C for 10 s, 72℃ for 40 s, 95℃ for 30 s, 65℃ for 30 s, and 95℃ for 30 s.

2.10 | Inoculation test

CMV-Y and CMVΔ2b inoculated *N. benthamiana* leaves were ground in 0.1 M phosphate buffer (pH 7.0) and carborundum powder was used to mechanically inoculate tomato ‘S8’ and *N. benthamiana* seedlings at the second or third true leaf stage. Uninoculated plants were used as healthy controls. At 35 dpi, CP accumulation in uninoculated upper leaves was investigated with anti-CP polyclonal antibody in a double antibody sandwich enzyme-linked immunosorbent assay (DAS-ELISA). CMV-Y genomic RNA was detected with a primer pair reported in Atarashi et

al. (2020) by RT-PCR. Mean and SE of absorbance values at 405 nm of samples from at least six independent plants per genotype were calculated. The susceptibility threshold was set as 3× the mean value of healthy controls.

2.11 | Yeast complementation assay

This yeast complementation assay was based on assays from previous studies (Gauffier et al. 2016; Kuroiwa et al. 2023). The cDNA of each *eIF4E1* allele (*SL-eIF4E1*, *Ath-eIF4E1*, or *9DEL-eIF4E1*) was cloned into the p424 plasmid using Gateway technology (ThermoFisher). The p424-RfA empty vector was used as a negative control and p424 + pvr^{2+} as a positive control. The plasmids were transformed into *S. cerevisiae* strain *JO55*. Transformants were initially selected on appropriate nutrient drop-out medium containing glucose to determine whether the 9DEL-eIF4E1 expressed from the plasmids could complement the wild-type *SL-eIF4E1* or *Ath-eIF4E1*. The assay was carried out with a 16-h light and 20°C / 8-h dark 16°C cycle.

3 | RESULTS

3.1 | Both eIF4E1 and the 9DEL variant binds to RSS 2b protein in Y2H assay

The in-frame 9-nucleotide deletion mutation of eIF4E1 (*9DEL*), but not the out-of-frame mutation containing a single-nucleotide insertion (*1INS*), enhanced resistance to CMV (Atarashi et al. 2020). This suggests that the mutant eIF4E1 protein expressed from *9DEL* interferes with specific CMV proteins. To test this hypothesis, we conducted a yeast two-hybrid (Y2H) assay to analyze interactions between wild-type or *9DEL*-mutated eIF4E1 and CMV proteins (CP, MV, and 2b). Yeast transformants expressing either wild-type eIF4E1 or the *9DEL*-derived mutant interacted with 2b, as indicated by growth on quadruple-drop medium (Figure 1a). To validate the interaction assay, we used a known interactor pair as a positive control: soybean eIF4E and the VPg protein of soybean mosaic virus (SMV). Co-expression of these proteins confirmed their interaction in the Y2H system (Figure S1a). Next, we examined the binding specificity of eIF4E1 and 9DEL-eIF4E1 to different variants of 2b. Initially, we used R2b derived from CMV strain CM95R, a subgroup I isolate known for relatively high RNA silencing suppressor activity. We additionally tested Y2b and HL2b, derived respectively from CMV-Y and CMV-HL (lily isolate), both of which also belong to subgroup I. Although Y2b shares similar characteristics to R2b, HL2b exhibits distinct properties, including reduced toxicity to *E. coli* compared to the other variants (Goto et al. 2007; Sueda et al. 2010). Both eIF4E1 variants interacted with Y2b (Figure S1b) but failed to bind HL2b (Figure 1a). Fny2b (from CMV-Fny) (Gao

et al. 2021) is identical in amino acid sequence to Y2b and is therefore expected to interact similarly with the eIF4E1 variants. HL2b differs from R2b and Y2b by unique amino acid substitutions at five positions (Figure 1b), some of which likely explain its inability to interact with eIF4E1 and 9DEL-eIF4E1. Because these substitutions are dispersed throughout the 2b coding region, identifying which residues are responsible for the difference in binding affinity could reveal regions within 2b essential for eIF4E1 interaction. To address this, we generated R2b point mutants, each individually substituted at one of the five amino acid positions with the corresponding residue from HL2b (Figure 1c). The R2b mutants harboring substitutions at the C-terminal residues 94 and 104 lost affinity to eIF4E1. Conversely, HL2b mutants carrying the reciprocal substitutions at residues 94 and 104 regained affinity to eIF4E1. Finally, an R2b mutant carrying a deletion that included the C-terminal region encompassing residues 94 and 104 also lost binding to eIF4E1, supporting the conclusion that these two C-terminal residues are critical for the interaction between 2b and eIF4E1 proteins.

3.2 | Confirmation of eIF4E1 and 9DEL-eIF4E1 interaction with R2b using a split-luciferase complementation

To validate the interactions between eIF4E1 variants and R2b, we conducted a split-luciferase complementation assay. In this assay, R2b was fused to either the N-terminal or C-terminal fragment of luciferase, while eIF4E1, 9DEL-eIF4E1, and potato virus X (PVX) coat protein (CP; negative control) were fused exclusively to the complementary N-terminal luciferase fragment. Interaction between fusion proteins brings these fragments into close proximity, reconstituting active luciferase and generating detectable chemiluminescence. These fusion constructs were transiently expressed in *N. benthamiana* leaves via agroinfiltration. Chemiluminescent signals were specifically detected in leaf areas co-expressing R2b with eIF4E1 or 9DEL-eIF4E1, but not in areas co-expressing the negative control PVX CP with these proteins (Figure 2). Additionally, consistent with previous reports describing homodimerization of 2b (Chen et al. 2008b), strong chemiluminescence was observed in leaf tissues co-expressing R2b fused separately to each luciferase fragment (Figure 2). The quantification of the luciferase intensity revealed a slightly higher signal in the R2b × eIF4E1 interaction compared to R2b × 9DEL-eIF4E1; however, the difference was not statistically significant according to Tukey's HSD test ($p < 0.05$) (Figure 2). These results clearly indicate that R2b physically interacts with both wild-type eIF4E1 and the mutant protein derived from 9DEL in plant cells.

3.3 | 9DEL-eIF4E1 binding partially inhibits the RSS activity of 2b

If 9DEL-eIF4E1 increased resistance to CMV is attributed to its interaction with 2b, 9DEL-eIF4E1 binding could negatively affect 2b's function in CMV infection. To examine this possibility, we tested the effect of 9DEL-eIF4E1 on the RSS activity of 2b. GFP and 2b were transiently expressed either alone or in combination with 9DEL-eIF4E1 or eIF4E1 by agroinfiltration into *N. benthamiana* leaves. Fluorescence was quantified using ImageJ, and the highest fluorescence was observed in leaf regions co-producing GFP and R2b, demonstrating the effective RSS activity of 2b in the absence of 9DEL-eIF4E1 or eIF4E1. Fluorescence intensity tended to decrease in the presence of 9DEL-eIF4E1, whereas wild-type eIF4E1 had little effect (Figure 3a, b). However, the difference between 9DEL-eIF4E1 and wild-type eIF4E1 was not statistically significant (Tukey's HSD test, $p = 0.313$), despite both proteins being capable of binding to R2b. Consistently, GFP protein and mRNA levels were reduced in the presence of 9DEL-eIF4E1 (Figure 3c, d), although the reduction in mRNA levels was not statistically significant compared to wild-type eIF4E1 (Figure 3d). Furthermore, no significant differences were observed in the relative mRNA levels of 2b, 9DEL-eIF4E1, and eIF4E1 (Figure 3e, f), suggesting that the inhibitory effect of 9DEL-eIF4E1 is likely post-translational. These findings raise the possibility that 9DEL-eIF4E1 may attenuate the RSS activity of 2b, which could contribute to the observed resistance to CMV.

3.4 | 2b is a pathogenicity determinant of CMV, essential for efficient systemic infection in tomato plants

Because 9DEL-eIF4E1 binding to 2b may negatively affect its function, we investigated the role of 2b in CMV virulence using CMVΔ2b, a mutant strain lacking 2b. Wild-type parental tomato ('S8') and *N. benthamiana* plants were inoculated with CMV-Y or CMVΔ2b. One month post-inoculation, CMV-Y-inoculated S8 plants exhibited clear symptoms, including leaf yellowing, whereas CMVΔ2b-inoculated S8 plants showed no visible symptoms. Consistently, CP was detected by ELISA in non-inoculated upper leaves of CMV-Y-inoculated S8 plants but not in CMVΔ2b-inoculated S8 plants (Figure 4a). In contrast, CMVΔ2b-inoculated *N. benthamiana* plants developed symptoms and accumulated CP (Figure 4a). These results demonstrate that the requirement of 2b for systemic infection varies among plant species. Notably, in tomato, 2b is strictly necessary for systemic infection, whereas CMVΔ2b retained systemic infectivity in *N. benthamiana* in this experiment. CMVΔ2b can also systemically infect other hosts, such as *N. tabacum* and *Arabidopsis thaliana*. Thus, 2b is particularly critical for CMV pathogenicity in tomato, highlighting it as an effective target to reduce CMV virulence in this host.

3.5 | Endogenous 9DEL-eIF4E1 accumulates in tomato plants and fails to complement eIF4E-defective yeast

We confirmed the accumulation of endogenous 9DEL-eIF4E1 protein in tomato plants infected with CMV. Protein accumulation was compared between *9DEL* and wild-type 'S8' tomato plants infected with either CMV-Y or CMV-2bΔC, a mutant lacking the C-terminal region of 2b, which is important for interacting with 9DEL-eIF4E1. Western blotting was performed using specific antibodies against CMV CP, tomato eIF4E1, and eIF4E2 (Figure 4b). The 9DEL-eIF4E1 protein accumulated in CMV-Y- and CMV-2bΔC-infected *9DEL* plants, although it accumulated at significantly lower levels than wild-type eIF4E1 in 'S8' plants, suggesting that 9DEL-eIF4E1 may contribute to disrupting 2b function through direct binding and impair CMV virulence. Consistently, CP accumulation was lower in *9DEL* plants than in 'S8' plants. We assessed the canonical function of eIF4E using a yeast complementation assay. Wild-type eIF4E1 complemented the growth defect of yeast lacking endogenous eIF4E, whereas 9DEL-eIF4E1 did not (Figure 5a), indicating that the canonical function of eIF4E is disrupted in the 9DEL-eIF4E1 protein.

4 | DISCUSSION

Natural mutations in genes encoding eIF4E and other translation-related factors account for nearly half of all known virus resistance resources in plants (Zlobin and Taranov 2023) and offer a major strategy for combating plant viral infections. Typically, such resistance conferred by natural eIF4E mutations arises from a loss of function of eIF4E, a susceptibility factor required for viral infection and replication (Zhou et al. 2014; Gao et al. 2018; Zhao et al. 2018; Shukla et al. 2022; Yoon et al. 2020; Yu et al. 2020). A loss-of-function mutant of eIF4E in Arabidopsis is resistant to CMV (Yoshii et al. 2004). This mutation prevents the virus from exploiting eIF4E and results in recessive resistance that is expressed only in homozygous individuals lacking the wild-type eIF4E. Previously, we showed that tomato plants with artificially mutated eIF4E1 are resistant to CMV (Atarashi et al. 2020), but the mechanism appears to differ from that conferred by natural eIF4E mutations. While natural resistance is typically associated with loss-of-function alleles that prevent virus–host factor interaction, the 9DEL-eIF4E1 allele contains a small in-frame deletion that produces a stable mutant protein capable of interfering with the function of the CMV 2b protein. CMV resistance in *9DEL* plants is achieved through eIF4E1-9DEL, whereas susceptible 1INS plants have disrupted eIF4E1 function (Atarashi et al. 2020). In our study, the yeast complementation assay suggests that 9DEL-eIF4E lost the canonical function of eIF4E (Figure 5a), yet this loss of function cannot explain the observed CMV resistance.

Here, we tested our hypothesis that 9DEL-eIF4E1 enhances resistance by actively interfering with CMV infection and replication. Our analyses support this hypothesis and reveal the mechanism by which 9DEL inhibits CMV proliferation.

Among the CMV proteins tested (three 2b variants, MP, and CP), Y2H suggested a potential interaction specifically between 9DEL-eIF4E1 and 2b (Figure 1a). Notably, Y2H revealed the critical role of the 2b C-terminal region, as mutations in this region disrupted the interaction (Figure 1b, c). To confirm our findings, we used split-luciferase complementation assay and found specific interactions between 2b and both wild-type eIF4E1 and 9DEL-eIF4E1 in agroinfiltrated leaves of *N. benthamiana* (Figure 2). Luciferase intensity quantification indicated that eIF4E1 exhibited slightly stronger binding to R2b than 9DEL-eIF4E1; however, the difference was not significant, suggesting that both eIF4E1 and 9DEL-eIF4E1 retain binding affinity to 2b. These findings raise the possibility that the differential effects on RSS activity may result from functional interference by 9DEL-eIF4E1, rather than reduced interaction with 2b. Together, these data support the interaction between 9DEL-eIF4E1 and CMV 2b, underscoring its functional significance in viral dynamics.

The interaction between 9DEL-eIF4E1 and R2b discovered in this study likely underlies CMV resistance in 9DEL plants. To determine whether 9DEL-eIF4E1 inhibits 2b functions critical for CMV virulence, we examined its effect on 2b RSS activity. Both wild-type eIF4E1 and 9DEL-eIF4E1 bound to 2b (Figures 1 and 2), but 9DEL-eIF4E1 tended to reduce RSS activity compared to wild-type eIF4E1 (Figure 3), although this difference was not statistically significant. Using an inoculation test with CMVΔ2b, we found that 2b is essential for systemic CMV infection in tomato (Figure 4a), aligning with related studies on the involvement of 2b in CMV systemic infection (Lewsey et al. 2009; Zhou et al. 2014; Khaing et al. 2020b). Beyond RSS suppression, 2b is known to interfere with plant defense-related hormone signaling, such as salicylic acid and jasmonic acid pathways (Wu et al. 2017; Ji et al. 2021; Arinaitwe et al. 2023; Crawshaw et al. 2024; Zhang et al. 2024) and to interact with autophagy-related processes in CMV infection (Jeon et al. 2017; Shukla et al. 2022; Tong et al. 2023), which play a recognized role in antiviral defense (Nakahara et al. 2012; Yang et al. 2020). Given these diverse functions, 9DEL-eIF4E1 may interfere not only with RSS activity but also with other 2b-mediated processes involved in CMV pathogenicity.

This study highlights the importance of 2b in CMV infection and resistance, as mutations in 2b have been shown to alter viral virulence in *A. thaliana* and *N. benthamiana* (Zhang et al. 2006; Goto et al. 2007; Lewsey et al. 2009; Sueda et al. 2010; Khaing et al. 2020b). Collectively, our findings suggest that 9DEL-eIF4E1 enhances CMV

resistance in tomatoes carrying the *9DEL* allele by binding to 2b and inhibiting its multiple functions (Figure 5b). In this study, we found that both wild-type eIF4E1 and its in-frame deletion mutant, 9DEL-eIF4E1, bind to the CMV 2b protein. Subsequent experimental results indicated that 9DEL-eIF4E1 expressed from the in-frame mutant allele attenuates CMV virulence by inhibiting the functions of 2b. However, in our experiments, wild-type eIF4E1 protein did not exhibit inhibitory activity against 2b. Moreover, tomatoes carrying a knockout mutation of eIF4E1 do not show increased resistance to CMV (Atarashi et al. 2020). These findings suggest that the in-frame deletion mutation endowed the mutant eIF4E1 protein with a novel ability to inhibit 2b, thereby contributing to enhanced CMV resistance that cannot be achieved by knockout mutations. Similar cases have previously been reported, where in-frame mutations resulted in novel or enhanced desirable traits, such as virus resistance conferred by specific amino acid substitutions in eIF4E alleles providing broader resistance to potyviruses compared to complete knockout alleles (Charron et al. 2008; Piron et al. 2010; Poulicard et al. 2016; Nekrasov et al. 2017; Bastet et al. 2018), and powdery mildew resistance conferred by specific in-frame mutations in MLO genes (Nekrasov et al. 2017). Therefore, utilizing targeted in-frame mutations represents a promising breeding strategy for developing crops with novel and beneficial traits.

5 | CONCLUSIONS

This study suggests a novel mechanism of partial resistance to CMV in tomatoes carrying the *9DEL* allele of eIF4E1, distinct from that of classical recessive resistance caused by natural eIF4E mutations in Arabidopsis. The 9DEL-eIF4E1 protein actively inhibits CMV infection by binding to the viral 2b protein and disrupts its functions, including RSS activity, which is crucial for CMV pathogenicity. These findings provide valuable insights into plant–virus interactions and offer new strategies for developing virus-resistant crops.

AUTHOR CONTRIBUTIONS

K.S.N., C.K., and H.A. conceived and designed the research. S.G., A.K., M.S.A., A.Y., M.S., K.M., and K.S.N. performed the experiments and analyzed the data. S.G. and A.K. wrote the manuscript. K.S.N. and M.S.A. edited the manuscript. All authors read and approved of the final manuscript.

ACKNOWLEDGMENTS

The authors thank Dr. Jean-Luc Gallois and Dr. Kyoka Kuroiwa for conducting the yeast eIF4E complementation assay, providing antibodies against eIF4Es, and reviewing the manuscript. This research was supported by JSPS KAKENHI (Grant Number JP22H02343).

CONFLICT OF INTEREST STATEMENT

The authors declare that they have no conflict of interest to disclose.

Data availability statement

The data that support the findings of this study are available from the corresponding author upon reasonable request.

REFERENCES

Arinaitwe W, Tungadi TD, Pate AE, Joyce J, Baek E, Murphy AM, Carr JP (2023) Induction of aphid resistance in tobacco by the cucumber mosaic virus CMVΔ2b mutant is jasmonate-dependent. *Mol Plant Pathol* 24: 391–395

Atarashi H, Jayasinghe WH, Kwon J, Kim H, Taninaka Y, Igarashi M, Ito K, Yamada T, Masuta C, Nakahara KS (2020) Artificially Edited Alleles of the Eukaryotic Translation Initiation Factor 4E1 Gene Differentially Reduce Susceptibility to Cucumber Mosaic Virus and Potato Virus Y in Tomato. *Front Microbiol* 11: 564310

Bastet A, Lederer B, Giovinazzo N, Arnoux X, German-Retana S, Reinbold C, Brault V, Garcia D, Djennane S, Gersch S, Lemaire O, Robaglia C, Gallois JL (2018) Trans-species synthetic gene design allows resistance pyramiding and broad-spectrum engineering of virus resistance in plants. *Plant Biotechnol J* 16: 1569–1581

Bastet A, Zafirov D, Giovinazzo N, Guyon-Debast A, Nogué F, Robaglia C, Gallois JL (2019) Mimicking natural polymorphism in eIF4E by CRISPR-Cas9 base editing is associated with resistance to potyviruses. *Plant Biotechnol J* 17: 1736–1750

Charron C, Nicolaï M, Gallois JL, Robaglia C, Moury B, Palloix A, Caranta C (2008) Natural variation and functional analyses provide evidence for co-evolution between plant eIF4E and potyviral VPg. *Plant J* 54: 56–68

Chen H, Zou Y, Shang Y, Lin H, Wang Y, Cai R, Tang X, Zhou JM (2008a) Firefly luciferase complementation imaging assay for protein-protein interactions in plants. *Plant Physiol* 146: 368–376

Chen HY, Yang J, Lin C, Yuan YA (2008b) Structural basis for RNA-silencing suppression by Tomato aspermy virus protein 2b. *EMBO Rep* 9: 754–760

Crawshaw S, Murphy AM, Rowling PJE, Nietlispach D, Itzhaki LS, Carr JP (2024) Investigating the Interactions of the Cucumber Mosaic Virus 2b Protein with the Viral 1a Replicase Component and the Cellular RNA Silencing Factor Argonaute 1. *Viruses* 16: 676

Gao L, Luo J, Ding X, Wang T, Hu T, Song P, Zhai R, Zhang H, Zhang K, Li K, Zhi H (2020) Soybean RNA interference lines silenced for eIF4E show broad potyvirus resistance. *Mol Plant Pathol* 21: 303–317

Gao Y, Yang J, Zhang X, Chen A, Gu Z, Du Z (2021) The Weak Small RNA-Binding Activity of the 2b Proteins of Subgroup II Cucumber Mosaic Virus Strains Is Insufficient for RNA Silencing Suppression. *Front Microbiol* 12: 760937

Gao S, Lu J, Cheng X, Gu Z, Liao Q, Du Z (2018) Heterologous replicase from cucumoviruses can replicate viral RNAs, but is defective in transcribing subgenomic RNA4a or facilitating viral movement. *Viruses* 10: 590

Gauffier C, Lebaron C, Moretti A, Constant C, Moquet F, Bonnet G, Caranta C, Gallois JL (2016) A TILLING approach to generate broad-spectrum resistance to potyviruses in tomato is hampered by eIF4E gene redundancy. *Plant J* 85: 717–729

Goto K, Kobori T, Kosaka Y, Natsuaki T, Masuta C (2007) Characterization of Silencing Suppressor 2b of Cucumber Mosaic Virus Based on Examination of its Small RNA-Binding Abilities. *Plant Cell Physiol* 48: 1050–1060

Hirsch J, Moury B (2021) Cucumber Mosaic Virus (Bromoviridae). *Encyclopedia of Virology*. *Elsevier,* pp. 371–382

Jeon EJ, Tadamura K, Murakami T, Inaba J-I, Kim BM, Sato M, Atsumi G, Kuchitsu K, Masuta C, Nakahara KS (2017) rgs-CaM Detects and Counteracts Viral RNA Silencing Suppressors in Plant Immune Priming. *J Virol* 91: e00761-17

Ji M, Zhao J, Han K, Cui W, Wu X, Chen B, Lu Y, Peng J, Zheng H, Rao S, Wu G, Chen J, Yan F (2021) Turnip mosaic virus P1 suppresses JA biosynthesis by degrading cpSRP54 that delivers AOCs onto the thylakoid membrane to facilitate viral infection. *PLoS Pathog* 17**:** e1010108

Kataoka J, Masuta C, Takanami Y (1990) Complete nucleotide sequence of RNA1 of cucumber mosaic virus Y strain and evolutionary relationships among genome RNAs of the virus strains. *Jpn J Phytopathol* 56: 501–507

Khaing YY, Kobayashi Y, Takeshita M (2020a) The C-terminal region of the 2a protein and 2b protein of cucumber mosaic virus are involved in the induction of shoestring-like leaf blade in tomato. *Virus Res* 289: 198172

Khaing YY, Kobayashi Y, Takeshita M (2020b) The 2b protein and C-terminal region of the 2a protein indispensably facilitate systemic movement of cucumber mosaic virus in radish with supplementary function by either the 3a or the coat protein. *Virol J* 17: 49

Kim H, Shimura H, Sueda K, Masuta C (2022) Importin/Exportin-mediated nucleocytoplasmic shuttling of cucumber mosaic virus 2b protein is required for 2b's efficient suppression of RNA silencing. *PLoS Pathog* 18: e1010267

Kuroiwa K, Danilo B, Perrot L, Thenault C, Veillet F, Delacote F, Duchateau P, Nogué F, Mazier M, Gallois JL (2023) An iterative gene-editing strategy broadens eIF4E1 genetic diversity in Solanum lycopersicum and generates resistance to multiple potyvirus isolates. *Plant Biotechnol J* 21: 918–930

Kuroiwa K, Thenault C, Nogué F, Perrot L, Mazier M, Gallois JL (2022) CRISPR-based knock-out of eIF4E2 in a cherry tomato background successfully recapitulates resistance to pepper veinal mottle virus. *Plant Sci* 316: 111160

Lewsey M, Surette M, Robertson FC, Ziebell H, Choi SH, Ryu KH, Canto T, Palukaitis P, Payne T, Walsh JA, Carr JP (2009) The Role of the *Cucumber mosaic virus* 2b Protein in Viral Movement and Symptom Induction. *Mol Plant Microbe Interact* 22: 642–654

Masuta C, Inaba J, Shimura H (2012) The 2b proteins of *Cucumber mosaic virus* generally have the potential to differentially induce necrosis on *Arabidopsis*. *Plant Signal Behav* 7: 43–45

Matsuo K, Hong JS, Tabayashi N, Ito A, Masuta C, Matsumura T (2007) Development of Cucumber mosaic virus as a vector modifiable for different host species to produce therapeutic proteins. *Planta* 225: 277–286

Mazier M, Flamain F, Nicolaï M, Sarnette V, Caranta C (2011) Knock-down of both eIF4E1 and eIF4E2 genes confers broad-spectrum resistance against potyviruses in tomato. *PLoS One* 6**:** e29595

Mehla J, Caufield JH, Uetz P (2015) Mapping protein-protein interactions using yeast two-hybrid assays. *Cold Spring Harb Protoc* 2015: 442–452

Moury B, Lebaron C, Szadkowski M, Ben Khalifa M, Girardot G, Bolou Bi BA, Koné D, Nitiema LW, Fakhfakh H, Gallois JL (2020) Knock-out mutation of eukaryotic initiation factor 4E2 (eIF4E2) confers resistance to pepper veinal mottle virus in tomato. *Virology* 539: 11–17

Murota K, Shimura H, Takeshita M, Masuta C (2017) Interaction between Cucumber mosaic virus 2b protein and plant catalase induces a specific necrosis in association with proteasome activity. *Plant Cell Rep* 36: 37–47

Nakahara KS, Masuta C, Yamada S, Shimura H, Kashihara Y, Wada TS, Meguro A, Goto K, Tadamura K, Sueda K, Sekiguchi T, Shao J, Itchoda N, Matsumura T, Igarashi M, Ito K, Carthew RW, Uyeda I (2012) Tobacco calmodulin-like protein provides secondary defense by binding to and directing degradation of virus RNA silencing suppressors. *Proc Natl Acad Sci U S A* 109: 10113–10118

Nekrasov V, Wang C, Win J, Lanz C, Weigel D, Kamoun S (2017) Rapid generation of a transgene-free powdery mildew resistant tomato by genome deletion. *Sci Rep* 7: 482

Otagaki S, Arai M, Takahashi A, Goto K, Hong J-S, Masuta C, Kanazawa A (2006) Rapid induction of transcriptional and post-transcriptional gene silencing using a novel Cucumber mosaic virus vector. *Plant Biotechnol* 23: 259–265

Pagán I (2019) CHAPTER 16: Movement Between Plants: Vertical Transmission. Cucumber Mosaic Virus. *The American Phytopathological Society*, pp. 185–198

Palukaitis P (2019) CHAPTER 10: Genome Structure and Expression. Cucumber Mosaic Virus. *The American Phytopathological Society*, pp. 113–121

Palukaitis P, Roossinck MJ, Dietzgen RG, Francki RIB (1992) Cucumber MOSAIC Virus. *Adv Virus Res* 41: 281–348

Piron F, Nicolaï M, Minoïa S, Piednoir E, Moretti A, Salgues A, Zamir D, Caranta C, Bendahmane A (2010) An induced mutation in tomato eiF4E leads to immunity to two potyviruses. *PLoS One* 5: e11313

Poulicard N, Pacios LF, Gallois JL, Piñero D, García-Arenal F (2016) Human Management of a Wild Plant Modulates the Evolutionary Dynamics of a Gene Determining Recessive Resistance to Virus Infection. *PLoS Genet* 12: e1006214

Ryabov E V., Fraser G, Mayo MA, Barker H, Taliansky M (2001) Umbravirus Gene Expression Helps Potato leafroll virus to Invade Mesophyll Tissues and to be Transmitted Mechanically between Plants. *Virology* 286: 363–372

Scholthof KBG, Adkins S, Czosnek H, Palukaitis P, Jacquot E, Hohn T, Hohn B, Saunders K, Candresse T, Ahlquist P, Hemenway C, Foster GD (2011) Top 10 plant viruses in molecular plant pathology. *Mol Plant Pathol* 12: 938–954

Shan H, Chen D, Zhang R, Wang X, Li J, Wang C, Li Y, Huang Y (2023) Relationship between Sugarcane eIF4E Gene and Resistance against Sugarcane Streak Mosaic Virus. *Plants* 12: 2805

Shukla A, Hoffmann G, Kushwaha NK, López-González S, Hofius D, Hafrén A (2022) Salicylic acid and the viral virulence factor 2b regulate the divergent roles of autophagy during cucumber mosaic virus infection. *Autophagy* 18: 1450–1462

Sueda K, Shimura H, Meguro A, Uchida T, Inaba J ichi, Masuta C (2010) The C-terminal residues of the 2b protein of Cucumber mosaic virus are important for efficient expression in Escherichia coli and DNA-binding. *FEBS Lett* 584: 945–950

Sunpapao A, Nakai T, Dong F, Mochizuki T, Ohki ST (2009) The 2b protein of cucumber mosaic virus is essential for viral infection of the shoot apical meristem and for efficient invasion of leaf primordia in infected tobacco plants. *J Gen Virol* 90: 3015–3021

Suzuki M, Kuwata S, Kataoka J, Masuta C, Nitta N, Takanami Y (1991) Functional analysis of deletion mutants of cucumber mosaic virus RNA3 using an in vitro transcription system. *Virology* 183: 106–113

Takahashi H, Tabara M, Miyashita S, Ando S, Kawano S, Kanayama Y, Fukuhara T, Kormelink R (2022) Cucumber Mosaic Virus Infection in Arabidopsis: A Conditional Mutualistic Symbiont? *Front Microbiol* 12: 770925

Tatineni S, Hein GL (2023) Plant Viruses of Agricultural Importance: Current and Future Perspectives of Virus Disease Management Strategies. *Phytopathology* 113: 117–141

Tong X, Zhao JJ, Feng YL, Zou JZ, Ye J, Liu J, Han C, Li D, Wang XB (2023) A selective autophagy receptor VISP1 induces symptom recovery by targeting viral silencing suppressors. *Nat Commun* 14: 3852

Tungadi T, Groen SC, Murphy AM, Pate AE, Iqbal J, Bruce TJA, Cunniffe NJ, Carr JP (2017) Cucumber mosaic virus and its 2b protein alter emission of host volatile organic compounds but not aphid vector settling in tobacco. *Virol J* 14: 91

Wang R, Du Z, Bai Z, Liang Z (2017) The interaction between endogenous 30S ribosomal subunit protein S11 and Cucumber mosaic virus LS2b protein affects viral replication, infection and gene silencing suppressor activity. *PLoS One* 12**:** e0182459

Wu D, Qi T, Li WX, Tian H, Gao H, Wang J, Ge J, Yao R, Ren C, Wang XB, Liu Y, Kang L, Ding SW, Xie D (2017) Viral effector protein manipulates host hormone signaling to attract insect vectors. *Cell Res* 27: 402–415

Yang M, Ismayil A, Liu Y (2020) Autophagy in Plant-Virus Interactions. *Annu Rev Virol* 7: 403–419

Yoon Y-J, Venkatesh J, Lee J-H, Kim J, Lee H-E, Kim D-S, Kang B-C (2020) Genome Editing of eIF4E1 in Tomato Confers Resistance to Pepper Mottle Virus. *Front Plant Sci* 11: 1098

Yoshii M, Nishikiori M, Tomita K, Yoshioka N, Kozuka R, Naito S, Ishikawa M (2004) The Arabidopsis Cucumovirus Multiplication 1 and 2 Loci Encode Translation Initiation Factors 4E and 4G. *J Virol* 78: 6102–6111

Yu D, Liao L, Zhang J, Zhang Y, Xu K, Liu K, Li X, Tan G, Chen R, Wang Y, Liu X, Zhang X, Han X, Wei Z, Li C (2020) A novel, easy and rapid method for constructing yeast twohybrid vectors using In-Fusion technology. *Biotechniques* 64**:** 219–224

Zhang JR, Liu YM, Li D, Wu YJ, Zhao SX, Wang XW, Liu SS, Walling LL, Pan LL (2024) Viral proteins resolve the virus-vector conundrum during hemipteran-mediated transmission by subverting salicylic acid signaling pathway. *Nat Commun* 15: 9448

Zhang X, Yuan Y-R, Pei Y, Lin S-S, Tuschl T, Patel DJ, Chua N-H (2006) *Cucumber mosaic virus* -encoded 2b suppressor inhibits *Arabidopsis* Argonaute1 cleavage activity to counter plant defense. *Genes Dev* 20: 3255–3268

Zhao JH, Liu XL, Fang YY, Fang RX, Guo HS (2018) CMV2b-Dependent regulation of host defense pathways in the context of viral infection. *Viruses* 10: 618

Zhou LX, Tian YP, Ren LL, Yan ZY, Jiang J, Shi QH, Geng C, Li XD (2024) A natural substitution of a conserved amino acid in eIF4E confers resistance against multiple potyviruses. *Mol Plant Pathol* 25: e13418

Zhou T, Murphy AM, Lewsey MG, Westwood JH, Zhang HM, González I, Canto T, Carr JP (2014) Domains of the cucumber mosaic virus 2b silencing suppressor protein affecting inhibition of salicylic acid-induced resistance and priming of salicylic acid accumulation during infection. *J Gen Virol* 95: 1408–1413
Zhou Z, Bi G, Zhou JM (2018) Luciferase Complementation Assay for Protein-Protein Interactions in Plants. *Curr Protoc Plant Biol* 3: 42–50
Zlobin N, Taranov V (2023) Plant eIF4E isoforms as factors of susceptibility and resistance to potyviruses. *Front Plant Sci* 14: 1041868

FIGURE LEGENDS

Figure 1 The CMV R2b protein interacts with both eIF4E1 and 9DEL-eIF4E1 in yeast two-hybrid (Y2H) assay. (a) Interactions of eIF4E1 and 9DEL-eIF4E1 with CMV proteins CP, MP, R2b, and HL2b (2b proteins encoded by 2 different viral isolates). The *Saccharomyces cerevisiae* Y2H Gold strain was co-transformed with pGADT7 and pGBT9 fusions of these proteins. Growth of transformants was assessed on selective media (SD-LT and SD-LTHA). (b) Comparison of Y2b, R2b, and HL2b amino acid sequences. Key substitutions are color-coded: yellow for Y2b and R2b, indicating their similarity, and blue for the unique substitutions in HL2b. (c) The five positions targeted for point mutations to generate eight R2b and HL2b variants. These variants were fused to pGBT9 vectors, while eIF4E1 and 9DEL-eIF4E1 were fused to pGADT7 vectors and tested as above. The reproducibility of the results was confirmed in three independent experiments.

Figure 2 Confirmation of R2b interaction with eIF4E1 and 9DEL-eIF4E1 in a split luciferase complementation assay. Agrobacterium transformants carrying constructs encoding the N- and C-terminal fragments of luciferase fused to the target proteins (PVX CP and R2b fused to N- and R2b, eIF4E1, and 9DEL-eIF4E1 to C-terminal) were co-infiltrated into *Nicotiana benthamiana* leaves. Chemiluminescence images were captured at 2 dpi. Luminescence indicates interactions between the co-expressed proteins. The combinations with potato virus X (PVX) coat protein (CP) were used as negative controls. Integrated density of luciferase was quantified using ImageJ. Values marked with an asterisk (*) represent quantified integrated density (IntDen) from the respective infiltrated leaf regions. Among the tested combinations, the co-expression of R2b with eIF4E1 produced higher luminescence signal compared to R2b with 9DEL-eIF4E1. In contrast, PVX CP combinations produced minimal luminescence, confirming the specificity of the interaction.

Figure 3 *9DEL* partially inhibits 2b RNA silencing suppressor activity in *N. benthamiana* leaves. (a) GFP was transiently co-expressed with negative control (GUS), Flag-tagged 2b, or Flag-tagged 2b in the presence or absence

of Myc-tagged eIF4E1 or 9DEL-eIF4E1. (b) GFP fluorescence intensity quantified in ImageJ. (c) Western blotting to assess different protein levels. (d–f) Quantitative RT-PCR to assess the relative transcript accumulation of GFP, 2b, and eIF4E1. Error bars represent standard deviation from three independent biological replicates ($n = 3$). In (b) and (d–f), the same lowercase letters indicate no significant differences in Tukey's HSD test ($p < 0.05$).

Figure 4 Inoculation test of tomato plants with CMV-Y and its derivatives. (a) CMV-Y and CMVΔ2b were inoculated into 'S8' tomato plants (the parental line of *9DEL*, indicated with WT) and *N. benthamiana* plants. ELISA was performed at 35 dpi to determine CP accumulation in the uninoculated upper leaves. Data is presented as the mean ± standard error from multiple biological replicates ($n=3$). The same letters above bars indicate no significant differences ($p < 0.05$), as determined by one-way ANOVA followed by Tukey's HSD test. (b) Detection of endogenous eIF4E in *9DEL* tomato plants by western blotting. *9DEL* and 'S8' were inoculated with CMV-Y or CMV-2bΔC (a truncate of 2b lacking C-terminal region). Tomato eIF4E1, eIF4E2, 2b, and CP were detected using specific polyclonal antibodies. To confirm the specificity of the eIF4E antibodies, eIF4E1 and eIF4E2 knockout plants (generated by genome editing to introduce frameshift mutations) were used.

Figure 5 Functional analysis of mutant 9DEL-eIF4E1 and the proposed mechanism of CMV resistance. (a) Yeast complementation assay. Yeast strain J055 transformed with the p424 empty vector served as a negative control, while the resistance *eIF4E1* allele (pvr^{2+}) was used as a positive control. Wild-type 'S8' tomato *SL-eIF4E1*, tomato *9DEL-eIF4E1*, and *Arabidopsis thaliana Ath-eIF4E1* proteins were tested. (b) The diagram illustrates a potential mechanism for CMV resistance in CRISPR/Cas9-edited *9DEL* tomato plants. Our findings suggest that 9DEL-eIF4E1 interacts with 2b, which disrupts 2b function and confers resistance to CMV. CMVΔ2b is unable to cause systemic infection, highlighting the essential role of 2b in CMV systemic infection in tomato plants.

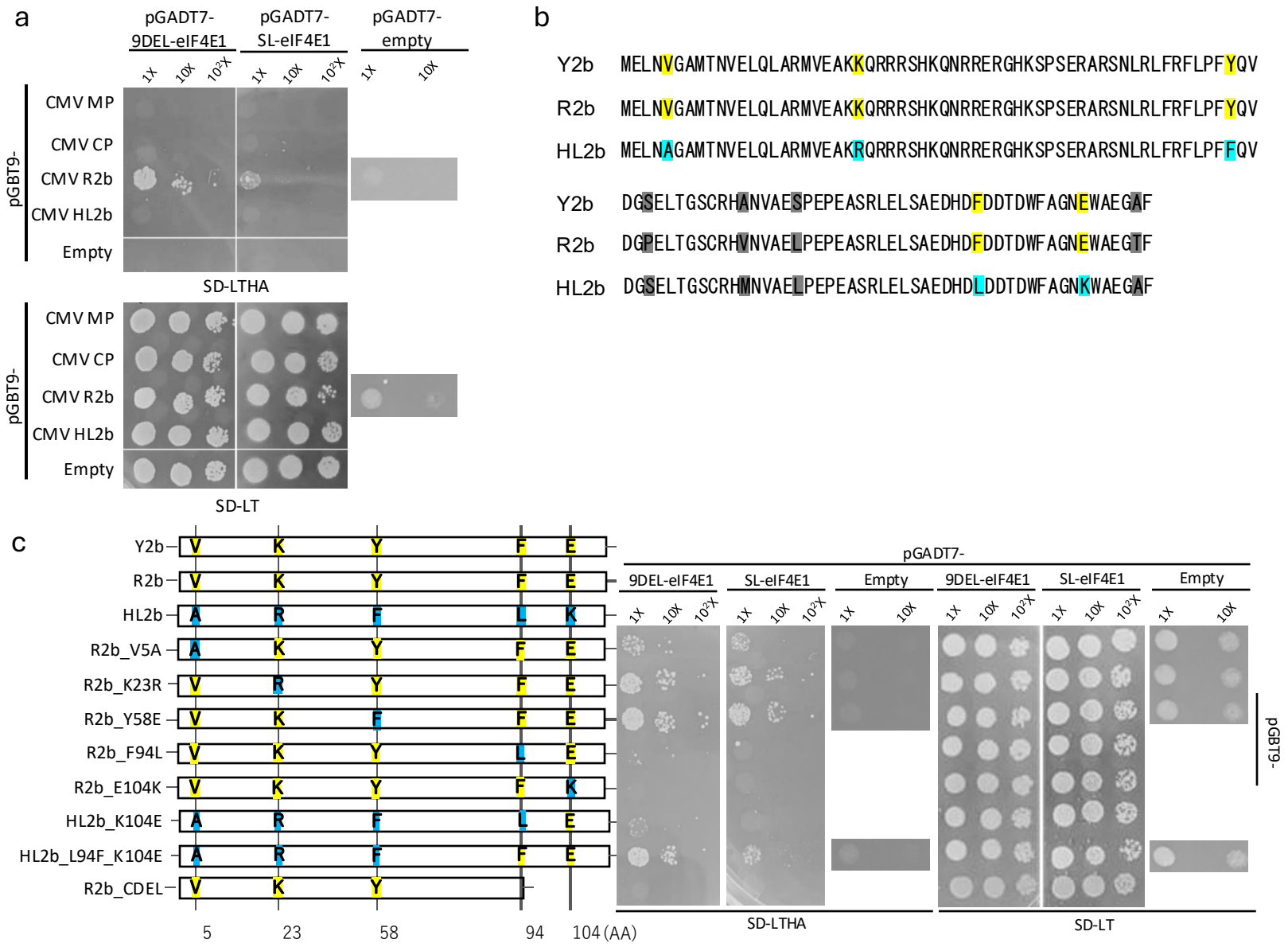
a
pGADT7-9DEL-eIF4E1
pGADT7-SL-eIF4E1
pGADT7-empty
1X
10X
10-2X
pGBT9-
CMV MP
CMV CP
CMV R2b
CMV HL2b
Empty
SD-LTHA
SD-LT
b
Y2b MELNVGAMTNVELQLARMVEAKKQRRRSHKQNRRERGHKSPSERARSNLRLFRFLPFYQV
R2b MELNVGAMTNVELQLARMVEAKKQRRRSHKQNRRERGHKSPSERARSNLRLFRFLPFYQV
HL2b MELNAGAMTNVELQLARMVEAKRQRRRSHKQNRRERGHKSPSERARSNLRLFRFLPFFQV
Y2b DGSELTGSCRHANVAESPEPEASRLELSAEDHDFDDTDWFAGNEWAEGAF
R2b DGPELTGSCRHVNVAELPEPEASRLELSAEDHDFDDTDWFAGNEWAEGTF
HL2b DGSELTGSCRHMNVAELPEPEASRLELSAEDHDLDDTDWFAGNKWAEGAF
c
Y2b
R2b
HL2b
R2b_V5A
R2b_K23R
R2b_Y58E
R2b_F94L
R2b_E104K
HL2b_K104E
HL2b_L94F_K104E
R2b_CDEL
5
23
58
94
104(AA)
pGADT7-
9DEL-eIF4E1
SL-eIF4E1
Empty
SD-LTHA
SD-LT
pGBT9-

Figure 1

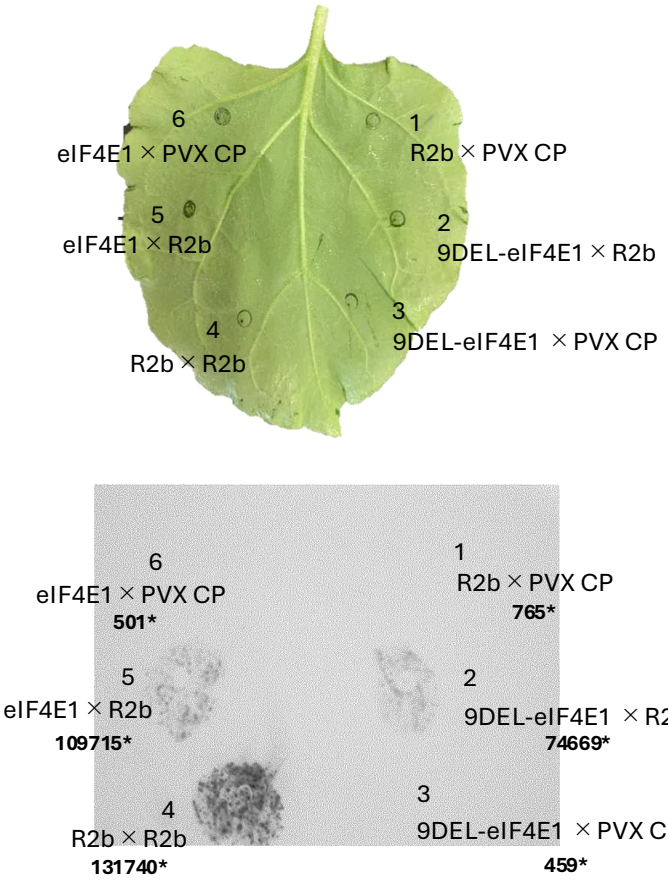
6
eIF4E1 × PVX CP
1
R2b × PVX CP
5
eIF4E1 × R2b
2
9DEL-eIF4E1 × R2b
3
9DEL-eIF4E1 × PVX CP
4
R2b × R2b
6
eIF4E1 × PVX CP
501*
1
R2b × PVX CP
765*
5
eIF4E1 × R2b
109715*
2
9DEL-eIF4E1 × R2b
74669*
4
R2b × R2b
131740*
3
9DEL-eIF4E1 × PVX CP
459*

Figure 2

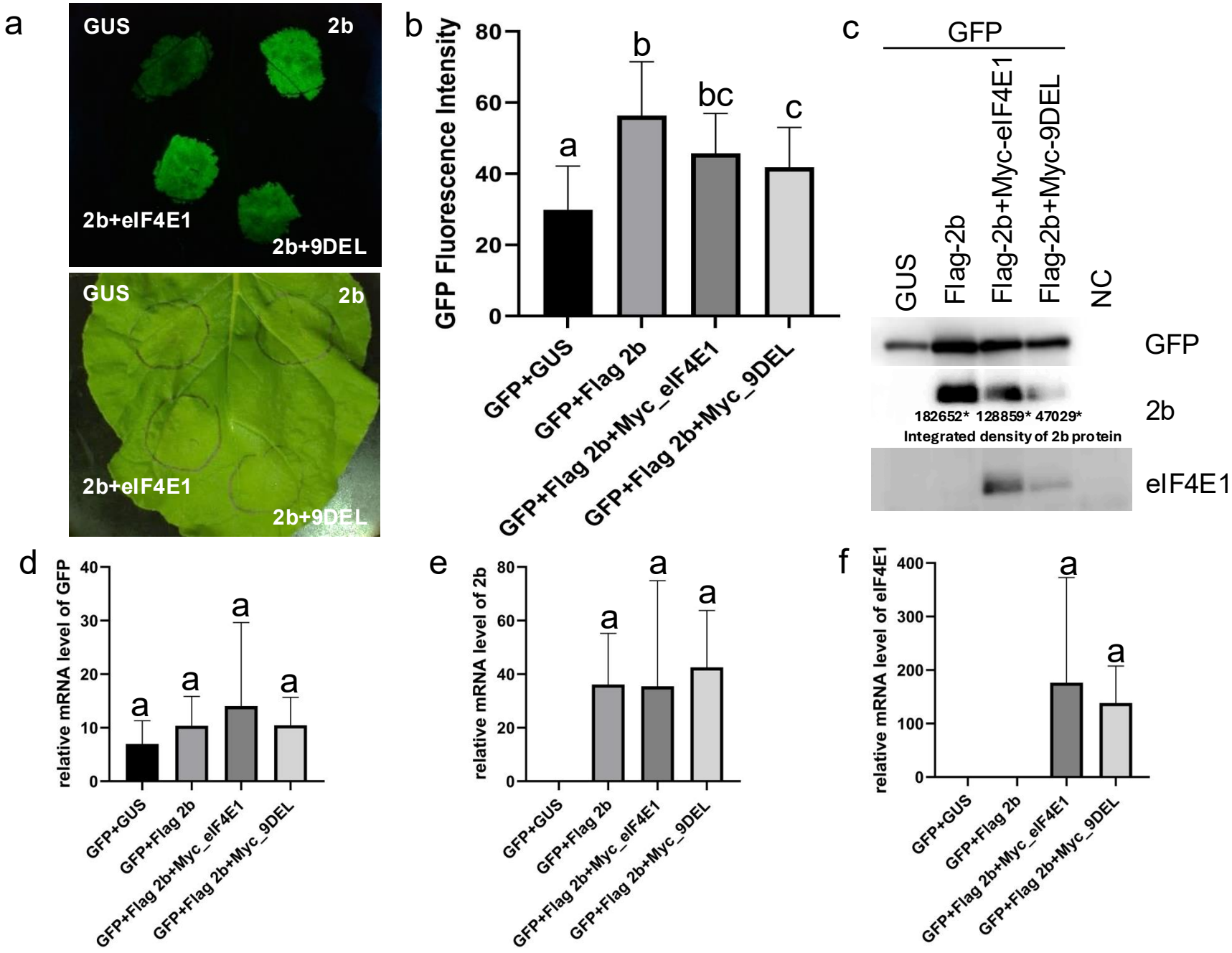
a
GUS
2b
2b+eIF4E1
2b+9DEL
GUS
2b
2b+eIF4E1
2b+9DEL
b
GFP Fluorescence Intensity
80
60
40
20
0
a
b
bc
c
GFP+GUS
GFP+Flag 2b
GFP+Flag 2b+Myc_eIF4E1
GFP+Flag 2b+Myc_9DEL
c
GFP
GUS
Flag-2b
Flag-2b+Myc-eIF4E1
Flag-2b+Myc-9DEL
NC
GFP
2b
182652* 128859* 47029*
Integrated density of 2b protein
eIF4E1
d
relative mRNA level of GFP
40
30
20
10
0
a
a
a
a
GFP+GUS
GFP+Flag 2b
GFP+Flag 2b+Myc_eIF4E1
GFP+Flag 2b+Myc_9DEL
e
relative mRNA level of 2b
80
60
40
20
0
a
a
a
GFP+GUS
GFP+Flag 2b
GFP+Flag 2b+Myc_eIF4E1
GFP+Flag 2b+Myc_9DEL
f
relative mRNA level of eIF4E1
400
300
200
100
0
a
a
GFP+GUS
GFP+Flag 2b
GFP+Flag 2b+Myc_eIF4E1
GFP+Flag 2b+Myc_9DEL

Figure 3

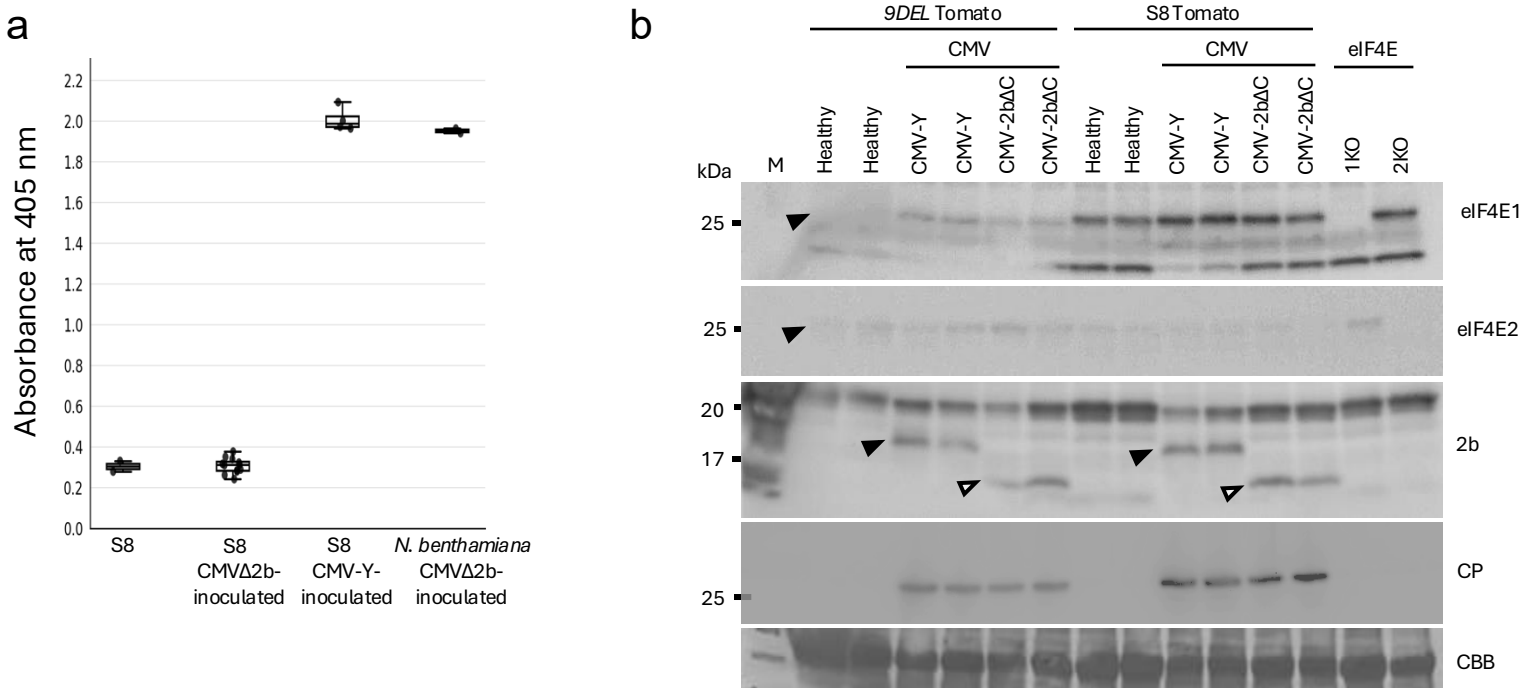
a
Absorbance at 405 nm
2.2
2.0
1.8
1.6
1.4
1.2
1.0
0.8
0.6
0.4
0.2
0.0
S8
S8 CMVΔ2b-inoculated
S8 CMV-Y-inoculated
N. benthamiana CMVΔ2b-inoculated
b
9DEL Tomato
S8 Tomato
CMV
CMV
eIF4E
Healthy
Healthy
CMV-Y
CMV-Y
CMV-2bΔC
CMV-2bΔC
Healthy
Healthy
CMV-Y
CMV-Y
CMV-2bΔC
CMV-2bΔC
1KO
2KO
kDa
M
25
25
20
17
25
eIF4E1
eIF4E2
2b
CP
CBB

Figure 4

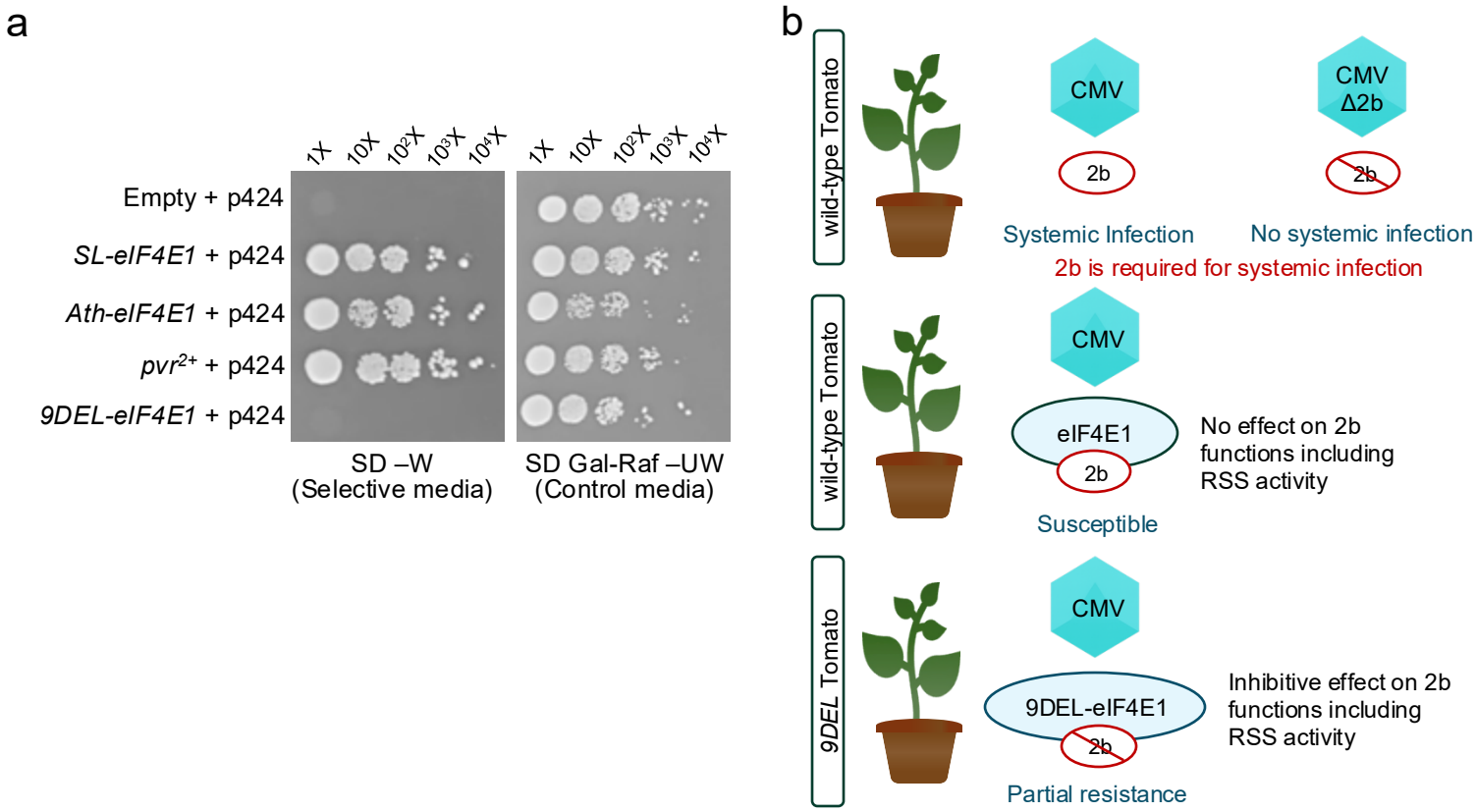
a
1X
10X
10²X
10³X
10⁴X
Empty + p424
SL-eIF4E1 + p424
Ath-eIF4E1 + p424
pvr²⁺ + p424
9DEL-eIF4E1 + p424
SD –W
(Selective media)
SD Gal-Raf –UW
(Control media)
b
wild-type Tomato
CMV
2b
CMV
Δ2b
2b
Systemic Infection
No systemic infection
2b is required for systemic infection
wild-type Tomato
CMV
eIF4E1
2b
No effect on 2b
functions including
RSS activity
Susceptible
9DEL Tomato
CMV
9DEL-eIF4E1
2b
Inhibitive effect on 2b
functions including
RSS activity
Partial resistance

Figure 5